Study the radiation attenuation properties of MgO/barite composite ceramics for photon shielding applications

D. A. Alorain[a], M. Elsafi[b,*], A. H. Almuqrin[a], S. Yasmin[c], M. I. Sayyed[d,e]
[a]*Department of Physics, College of Science, princess Nourah bint Abdulrahman University, P.O.Box 84428, Riyadh 11671, Saudi Arabia*
[b]*Physics Department, Faculty of Science, Alexandria University, 21511 Alexandria, Egypt.*
[c]*Department of Physics, Chittagong University of Engineering and Technology, Chattogram, Bangladesh*
[d]*Department of Physics, Faculty of Science, Isra University, Amman – Jordan*
[e]*Department of Nuclear Medicine Research, Institute for Research and Medical Consultations (IRMC), Imam Abdulrahman bin Faisal University (IAU), P.O. Box 1982, Dammam 31441, Saudi Arabia*

Five ceramic samples have been considered termed as S1, S2, S3, S4, and S5 on the purpose of radiation shielding. Ceramic sample S1 specifies pure MgO (100 wt %) with no other addition of Barite ($BaSO_4$), yet another samples S2, S3, S4, and S5 have been considered 10 wt %, 20 wt %, 30 wt %, and 50 wt % of Barite ($BaSO_4$) instead of MgO. Few shielding parameters such as linear attenuation coefficients (LAC), effective atomic number (Z_{eff}), equivalent atomic number (Z_{eq}) and radiation absorption ratio (RAR) were calculated through Geant4 code and experimental technique for the interest of evaluating the radiation shielding strength of the considered ceramic samples. The value of LAC of the considered ceramic samples via Experimental and Geant4 code were found a negligible difference. Considered ceramic samples S5 presents the most suitable radiation shielding capacity comprising rest of the ceramic samples according to the value of LAC for low energy. Considered ceramic sample S5 with the composition of [MgO (50%)-$BaSO_4$ (50%)] were provided lowest value of HVL, TVL, and MFP. Hence, the obvious concern is that greater amount of Barite ($BaSO_4$) lift up the shielding ability MgO ceramic in place of MgO.

(Received May 8, 2023; Accepted September 18, 2023)

Keywords: Ceramic, Magnesium oxide, Barite, Experimental technique, Geant4 code

1. Introduction

Gamma radiations are one of the types of ionizing radiations. Because of their extraordinarily high energy, they are able to penetrate matter to a significant degree. Because gamma photons (particularly those that have a high energy) are capable of easily penetrating biological organs, it is generally known that they pose a significant threat to both the people and the environment. Gamma radiations are known to have deleterious impact on the human body and to be capable of causing DNA and cell damage. In any facility, whether it be a nuclear one or a clinical one, there is a protocol that has to be adhered to, and among the most essential safety measures is the utilization of radiation shielding components [1-3]. Due to its efficient absorption capabilities, high density, low cost, high attenuation coefficients, and minimal maintenance requirements, lead composites have traditionally been extensively used in radiation shielding technologies [4]. However, latest research in the radiation shielding field has shown that lead composites have several disadvantages, including health risks owing to the lead's toxicity, poor mechanical qualities, and heaviness. Because of these difficulties as well as other disadvantages associated with these conventional materials, additional studies are required about the usefulness

* Corresponding author: dr.mabualssayed@gmail.com
https://doi.org/10.15251/DJNB.2023.183.1125

of shielding provided by various alternative materials. Recently, various new materials, such as ceramics, glasses, polymers, alloys, and nanomaterials have been produced for use as shielding materials [5-13]. Ceramics are attracting considerable interest for use as radiation shielding materials because to their great thermal stability, good mechanical characteristics, high corrosion resistance, superior capacity to absorb incoming radiation, and good thermal conductivity. Previous research has shown that the attenuation characteristics of ceramics have the potential to outperform those of other materials. Therefore, it is very important to conduct tests on the radiation attenuation characteristics of recently formed ceramics [14, 15].

In a brief, we reviewed the work that had been done in the past for the researchers who were interested in the radiation attenuation investigation for various types of ceramics. Asal et al. conducted research on the effectiveness of naturally bentonite clay-based ceramics in absorbing gamma photons [16]. Using point sources of Y-88, and Co-57, Cs-137, Am-251, the shielding capability of the materials that were investigated was analyzed and evaluated. Oto et al. [17] conducted research into the potential of ordinary ceramic and ceramics doped with molybdenum to shield gamma radiation. Ceramic incorporating 30% Mo exhibited better effective atomic numbers than other ceramics. The authors observed that an increase in the content of Mo resulted in a greater radiation shielding capabilities in the ceramics that were investigated. Sayyed et al [18] conducted research on the radiation shielding properties of bi-ferroic ceramics that contained carbon nanotubes. They found a relation between the amount of carbon nanotubes in the ceramics and the half value layer values. Mhareb et al. [19] shown that a ceramic containing $BaTiO_3$ that has been doped with Bi_2O_3 can be efficient for its shielding effectiveness. Hannachi et al [20] used Monte Carlo simulation and investigated the effect of WO_3, SiO_2 and ZnO on the attenuation factors of lead-free BTO perovskite ceramics. The linear attenuation coefficients for these ceramics were enhanced with the addition of WO_3 and ZnO, while they were decreased with adding SiO_2.

Chemical durability of glass system has enhanced with the lift up of MgO [21-[23]. Considering the radiation shielding utilization of barite (BaSO4) instead of lead oxide (PbO) in building construction is more suitable for having higher atomic number [24]. Barite ($BaSO_4$) is more suitable than lead [25] and tungsten [26] in radiation shielding. Having the Barite composite filler on Natural rubber (NR), epoxy and concrete have shown a good shielding ability in replace of traditional shielding material lead. In addition, because of few specific feature $BaSO_4$ is considered as a suitable filler such as non-toxicity, cost effectiveness, gotten from nature [27, 28].

Therefore, this study aims to fabricate a pioneer ceramic with the composition of $MgO/BaSO_4$ to evaluate the radiation shielding parameters using Geant4 code and Experimentaltechnique on the purpose of radiation shielding.

2. Materials and method

2.1. Ceramics fabrication

Samples were fabricated to study the radiation shielding properties. MgO and $BaSO_4$ were collected from local stores, as two powders with an average size of 50 μm. The EDX "energy dispersive x-ray analysis" was used to estimate the compositions percentage of both powder as reported in Table 1.The two powders were mixed and milled in the proportions shown in Table 2, after which a quantity of distilled water was added to obtain a homogeneous paste and put it in molds and let it dry at 100 ^{0}C for 24 hours. The dried mixture is inserted into a ball mill with the addition of 50% to 60% of the previous percentage of water. The ball mill is run for 70-90 min and the mixture taken out in molds, after which it is burned in electric furnace at 1050~1100 ^{0}C.

Table 1. The chemical composition of raw materials.

Oxides (%)	MgO	Barite
MgO	97.25	0.21
SiO_2	1.23	2.26
Al_2O_3	--	0.36
Fe_2O_3	--	0.17
CaO	1.52	0.07
SO_3	--	32.04
SrO	--	2.68
BaO	--	62.20

Table 2. The percentage of oxides in the present work for all prepared ceramics samples.

Ceramic Code	Oxide percentage (%)		Density ($g.cm^{-3}$)
	MgO	$BaSO_4$	
S1	100	0	3.579±0.016
S2	90	10	3.628±0.013
S3	80	20	3.679±0.020
S4	70	30	3.740±0.008
S5	50	50	3.857±0.009

2.2. Ceramics attenuation characteristics

The density of prepared composites were measured according to mass to volume law, where the sample was weighted and the radius (r) as well as the thickness (x) was calculated to evaluate the volume ($^4/_3 \pi r^3$). For the attenuation measurements, the experimental technique was used using an HPGe detector and different point sources [29-33]. The experimental mechanism depends on calibrating the detector first and choosing the appropriate position for the distance of the source from the detector, as well as the mechanism for placing the sample between them. Using Genie-2000 technique, the area under each estimated photopeak can be calculated whether the sample is present or not. From these photopeak values, the LAC can be calculated by Eq.1.

Geant4 code [34-36] was used in this study as a simulation technique to verify the experimental method, where the detector and point sources were simulated equivalent to the experimental work. Also, the sample was simulated with the percentage of each oxide. The sample was simulated between the source and the detector as shown in Figure 1.

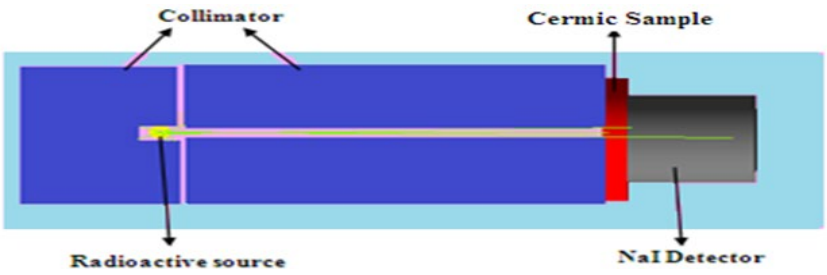

Fig. 1. Schematic diagram of the Geant4 simulation in this paper.

After simulation, the program was run with number of events 10^7 in the two cases of the pretence and removing the simulated ceramic sample, the product after each run was the peak related to the number of events as shown in Fig. 2.

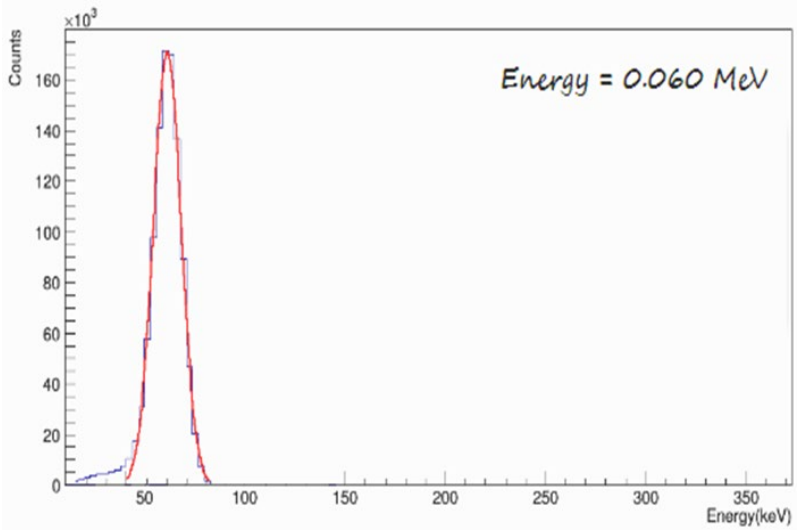

Fig. 2. Simulated spectrum in Geant4 at energy 0.06 MeV in case the pretence the ceramic sample.

The area under the peak can be calculated with helping ROOT technique [37, 38]. From these areas, the LAC can be calculated. The LAC defined as the probability of photon interactions with matter per unit path length and given by [39-41]:

$$LAC = \frac{-1}{x} \ln {}^{A}/_{A_0} \quad (1)$$

where, A and A_0 represents the Area under the peak in absence and present the ceramic sample using root technique. The spectrum was obtained in case without and with the ceramic layer at different energies (0.060, 0.662, 1.173 and 1.333 MeV). The simulated values of LAC for the present ceramic samples were compared with the results obtained from the experimental technique. The relative deviation between the two results calculated by:

$$Dev(\%) = \frac{LAC_{Geant4} - LAC_{Exper}}{LAC_{Exper}} \times 100 \quad (2)$$

The HVL can be estimated from the following equation [42, 43].

$$HVL = \frac{\ln 2}{\mu} \quad (3)$$

The radiation absorption ratio (RAR) is calculated from next equation [44-46].

$$RAR(\%) = [1 - \frac{A}{A_0}] \times 100 \quad (4)$$

3. Results and discussion

The obtained value of LAC of the considered ceramic samples were calculated using Geant4 code and Experimental technique. The variation of LAC of the considered ceramic samples against incident photon energy at 0.06, 0.66, 1.73, and 1.33 MeV were elaborately presented in Table 3. From this figure, it is very observable that the value of LAC of the considered ceramic samples were reduced upgrading the incident photon energy. As no difficulties has been found when the high intense photon passes through the absorber because of this reason the value of linear attenuation coefficients has turn out to be very minute comparing to low energy. Whereas, Compton scattering cross section diverse reversely with the incident photon energy.

Noteworthily, a very negligible variation has seen between the values of LAC of the considered ceramic samples obtained from Geant4 and Experimental technique. At energy 0.06 MeV, the value of linear attenuation coefficients (LAC) are - S1(0.8 cm^{-1}), S2(2.6 cm^{-1}), S3(4.5 cm^{-1}), S4(6.3 cm^{-1}), and S5(10.5 cm^{-1}) calculated by Geant4 code. Considered ceramic samples S2, S3, S4, and S5 provided 3.2 times, 5.5 times, 7.7 times, and 12.8 times greater value of linear attenuation coefficients (LAC) than considered ceramic samples S1. Again, the value of linear attenuation coefficients (LAC) are S1(0.275 cm^{-1}), S2(0.279 cm^{-1}), S3 (0.284 cm^{-1}), S4 (0.288 cm^{-1}), and S5(2.98 cm^{-1}) at energy 0.66 MeV. Hence, the studied ceramic samples have shown the value of LAC at energy 0.06 MeV is 3 times (S1), 10 times (S2), 16 times (S3), 22 times (S4), and 36 times (S5) greater value comprising the value of LAC at energy 0.66 MeV. As at low energy the photoelectric absorption process (PE) is the dominant but in the mediocre energy level Compton scattering (CS), and at high energy region pair production (PP) process has the dominant. However, considered ceramic samples S5 presented the most suitability for radiation shielding among the rest of the considered ceramic samples according to the value of linear attenuation coefficients (LAC) for low energy.

Table 3. The experimental and Geant4 results of LAC and relative deviation.

Ceramic Code	Energy (MeV)	Geant4 LAC values (cm^{-1})	Experimental LAC values (cm^{-1})	Dev (%)
S1	0.060	0.832	0.819	1.63
	0.622	0.275	0.269	2.22
	1.173	0.209	0.213	-1.79
	1.333	0.196	0.194	1.04
S2	0.060	2.657	2.598	2.25
	0.622	0.279	0.272	2.66
	1.173	0.211	0.201	4.98
	1.333	0.198	0.192	2.94
S3	0.060	4.536	4.499	0.83
	0.622	0.284	0.295	-3.82
	1.173	0.213	0.214	-0.48
	1.333	0.199	0.197	1.22
S4	0.060	6.474	6.299	2.78
	0.622	0.288	0.282	2.27
	1.173	0.215	0.221	-2.70
	1.333	0.201	0.199	1.13
S5	0.060	10.537	10.51	0.26
	0.622	0.298	0.292	2.13
	1.173	0.219	0.214	2.49
	1.333	0.205	0.201	2.05

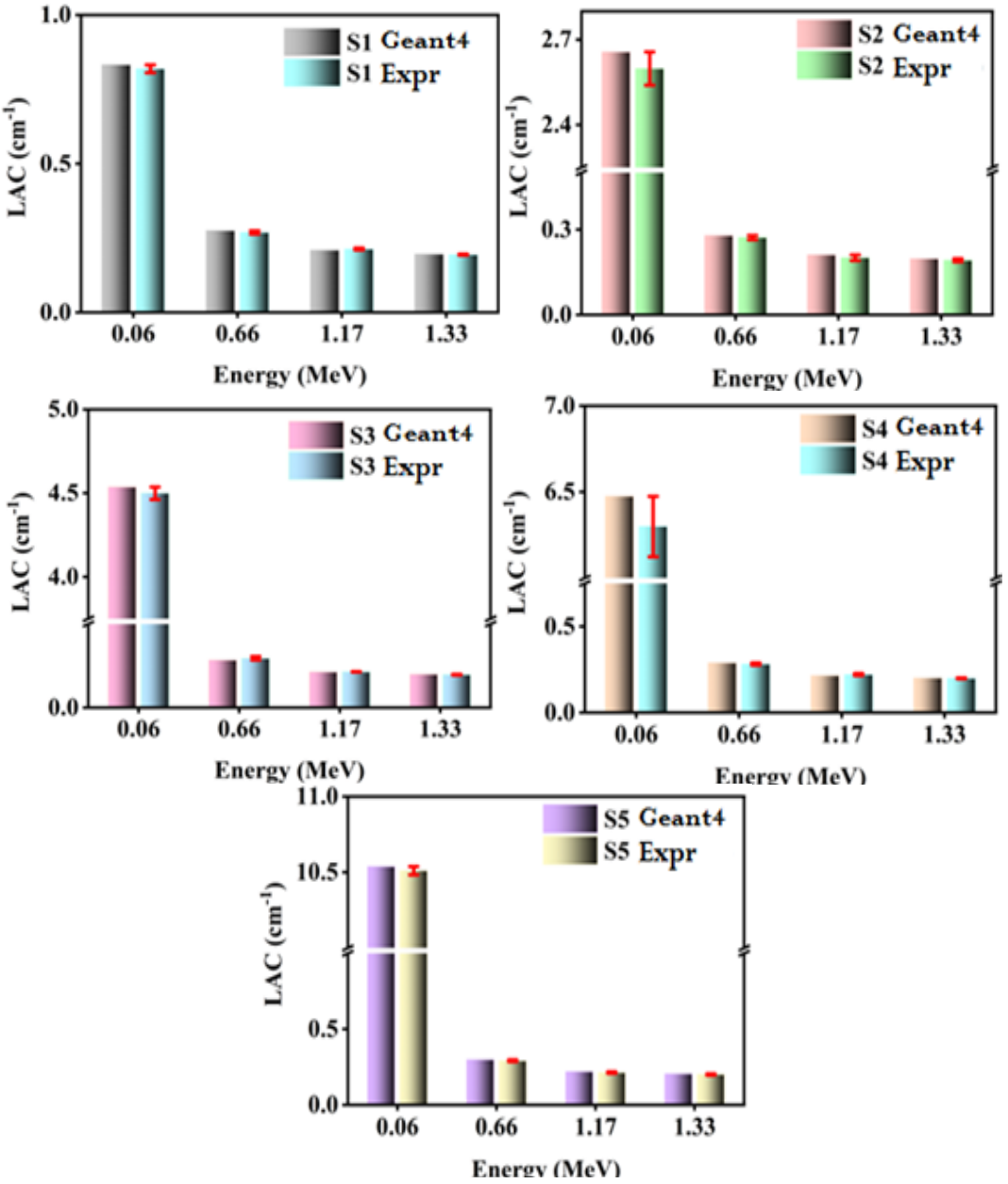

Fig. 3. The value of linear attenuation coefficients (LAC) of the considered ceramic samples according to energy.

As gamma emission is a continuous process, hence, the thickness of the absorber has played an essential role to reduce the impact of hazardous radiation. HVL in Fig. 4 can represent the requited value of the absorber that can reduce the intensity of the incident radiation fifty present and it's a linear attenuation coefficient value dependent parameter. The following decreasing trend were followed by the value of half value layer (HVL) of the considered ceramic samples as - S1(0.83 cm)> S2(0.26 cm)> S3(0.15 cm)> S4(0.11 cm)> S5(0.07 cm). Hence, according to the value of half value layer (HVL) - ceramic sample S1 (12.7 times), S2 (4 times), S3 (2.3 times), S4 (1.6 times) showed greater value than sample S5. From the composition of the considered samples it has been observed that sample S1 was pure MgO whereas the composition of sample S5 was [MgO (50%)-$BaSO_4$ (50%)]. It is clear concern that addition of Barite ($BaSO_4$) increase the shielding ability of the considered ceramic samples.

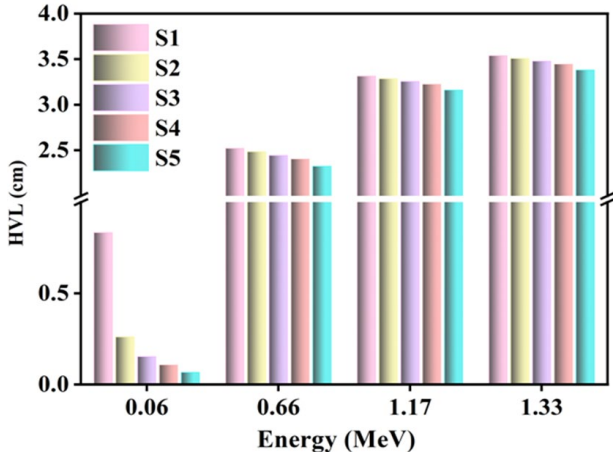

Fig. 4. The half value layer of the considered ceramic samples according to energy.

TVL is the analogous parameter like as HVL where the TVL represents the thickness of the absorber can reduce 90% of its incident radiation. That means when anybody use the TVL of the shield then only 10% of the incident radiation will pass through that absorber. The obtained value of the TVL of the considered ceramic samples has been graphed in Fig. 5. At energy 0.06 MeV, the value of TVL varies from 2.77 cm to 0.22 cm whereas at energy 1.33 MeV the value of TVL differs from 11.75 cm to 11.23 cm. It is vibrant that for lower energy good shielding ability has been provided by Sample S5.

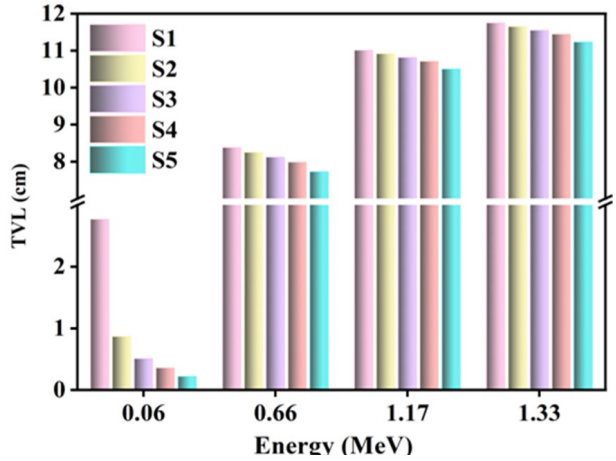

Fig. 5. The tenth value layer of the considered ceramic samples according to energy.

The average distance of two consecutive collusions is represented by the value of mean free path (MFP). When the value of mean free path (MFP) is found to be shorter than it indicates that because of collision more energy is absorbed consequently more photons are reduced. Fig. 6, is the graphed of the value of mean free path (MFP) of the considered ceramic samples against incident photon energy from 0.06 MeV to 1.33 MeV. The value of mean free path (MFP) varies for S1 (1.2 cm - 5.1 cm), S2 (0.4 cm - 5.1 cm), S3 (0.2 cm -5.0 cm), S4 (0 .2 cm - 5.0 cm), and S5 (0.1 cm - 4.9 cm). From these obtained values it is clear that considered ceramic sample S5 has shown the shortest value of mean free path (MFP) at energy 0.06 MeV, 0.66 MeV, 1.17MeV, and 1.33 MeV. As an illustration, at energy 0.66 MeV, the MFP values are S1 (1.2 cm), S2 (0.38 cm), S3 (0.22 cm), S4 (0.15 cm), and S5 (0.09 cm) when the concentrations of Barite ($BaSO_4$) on the ceramic samples are 0, 10, 20, 30, and 50 mol %, respectively. For all studied energies, the

enhancement of Barite ($BaSO_4$) in the considered ceramic samples provided a lessening value on mean free path (MFP).

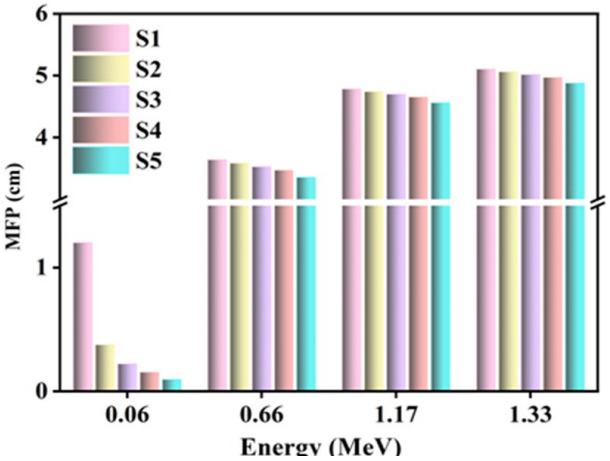

Fig. 6. The mean free path (MFP) of the considered ceramic samples according to energy.

One of the most promising shielding parameters is effective atomic number (Z_{eff}). The highest value of Z_{eff} of composite indicates the greater number of electrons per atom. It's well known that attenuation cross-section is sum up of photoelectric effect, Compton scattering, and pair production. Again, photoelectric effect is proportional to Z^{4-5}; Compton scattering is proportional to Z as well as pair production is proportional to Z^2 (where, Z represents the atomic number for single material and for compounds it is Z_{eff}). Below the energy of 0.1 MeV, photoelectric interaction is prevalent, yet at the energy range 0.1 MeV–1 MeV, photoelectric absorption is declined & Compton scattering is started dominant and also, the pair production is the most prime interaction at energy limit 1 MeV–15 MeV. The value of Z_{eff} of ceramic samples were calculated in the energy range between 0.015 MeV and 15 MeV through Experimental technique and Fig. 7, represents the graphical presentation of the value of Z_{eff} of the considered ceramic samples. Ceramic sample S1 contained only MgO, where another ceramic sample contained 10, 20, 30, and 50 mol % of Barite ($BaSO_4$) respectively in replace of MgO. Ceramic sample S5 having composition [50% MgO - 50% Barite ($BaSO_4$)] represented the greatest value of effective atomic number (Zeff) compared with rest of the considered ceramic samples. Moreover, the value of Z_{eff} of ceramic samples were increased suddenly at energy 0.04 MeV and they are S1(10.6), S2(29.8), S3(38.3), S4(43), and S5(48.1). That means with the enhancement of Barite ($BaSO_4$) uprise the shielding ability of considered ceramic samples.

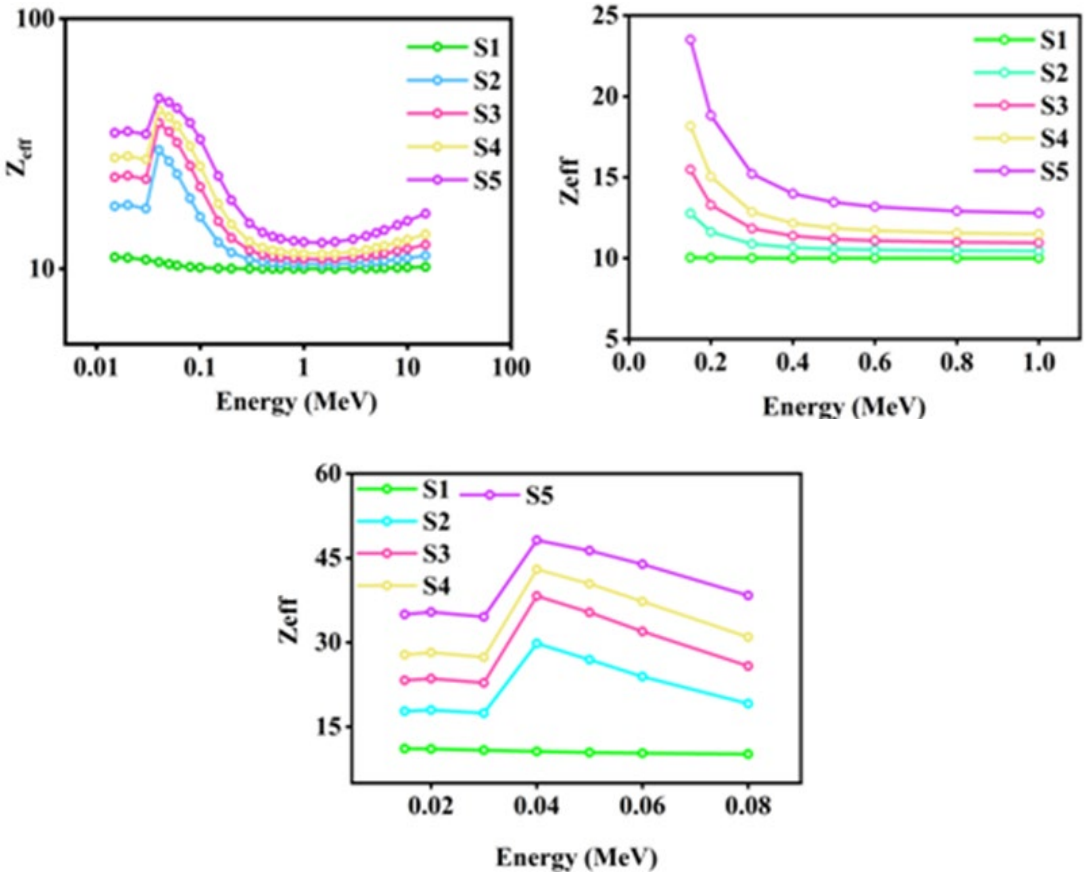

Fig. 7. The effective atomic number (Zeff) of the considered ceramic samples according to energy.

Within the energy region 0.015 MeV to 15 MeV, the value of equivalent atomic number (Zeq) of the considered ceramic samples were calculated using Experimentaltechnique. The value of equivalent atomic number (Zeq) of the considered ceramic samples is presented in Fig. 8. This graph shows that the value of Zeq grows gradually with the increase of Barite ($BaSO_4$) in place of decreasing MgO by 10, 20, 30, and 50 % respectively. Herein, ceramic sample S5 with the composition of [50 mol % MgO – 50 mol % Barite ($BaSO_4$)] showed the greatest value of equivalent atomic number (Zeq) comparing rest of the considered ceramic samples. There was a sudden increase in the value of Z_{eq} at energy 0.04 MeV, they were followed the increasing trend – S1(10.8) <S2(19.9) <S3(24.3) <S4(27.5) <S5(32.7). However, after 1 MeV, all ceramic samples started doing decreasing trend except samples S1. From this obtained graph, it is clear that with the enhancement of Barite (BaSO4) uprise the shielding ability of studied samples.

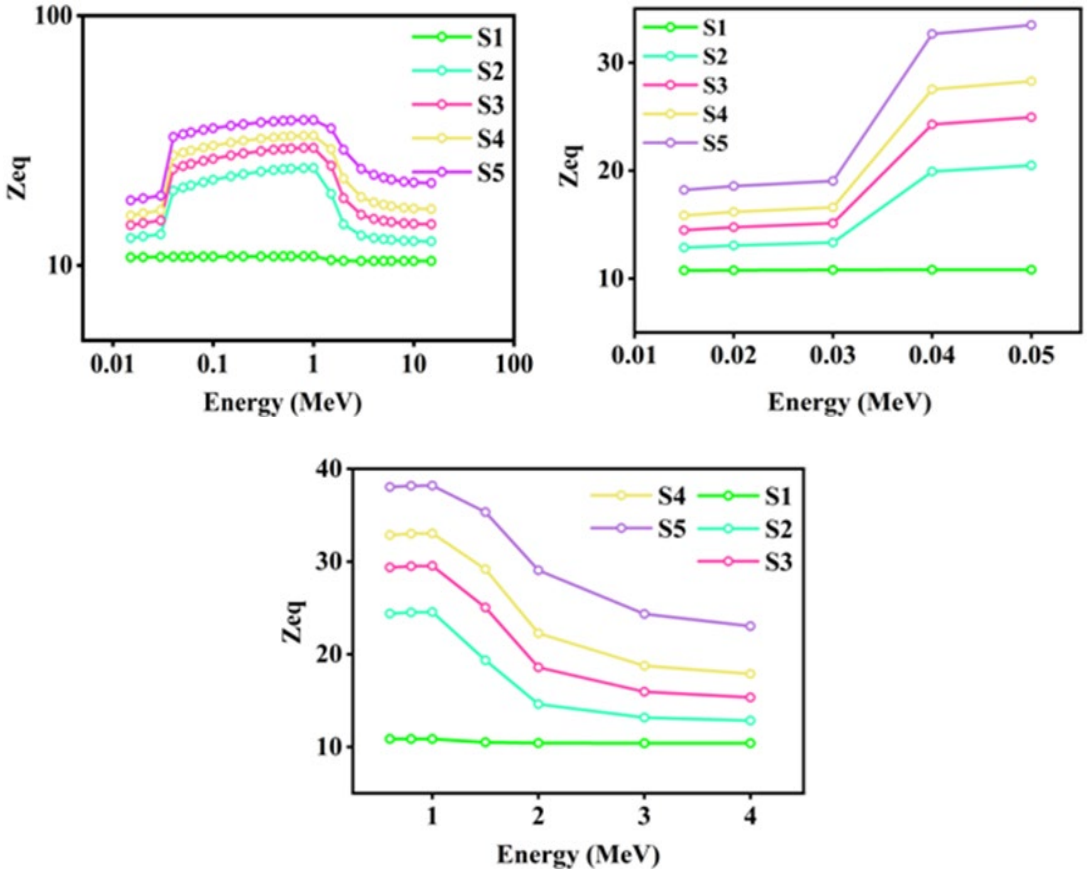

Fig. 8. The equivalent atomic numbers (Zeq)of the considered ceramic samples according to energy.

Radiation absorption ratio (RAR) is another most significant indicators of an absorber to specify the radiation shielding ability. It evaluates the number of photons absorbed by the shield. **Fig. 9.** graphed the radiation absorption ratio (RAR) of the considered ceramic samples S1, S2, S3, S4, and S5. At energy 0.06 MeV, the value of radiation absorption ratio (RAR) were S1 (34 %), S2 (73.5 %), S3 (89.7 %), S4 (96.1 %), and S5 (99.5 %) while the thickness of the absorber was 0.5 cm. That means ceramic sample S5 having thickness of 0.5 cm can absorb approximately all of the incident photons. Hence, the shielding capability of MgO ceramic is raised according to the higher amount of Barite ($BaSO_4$) in place of MgO.

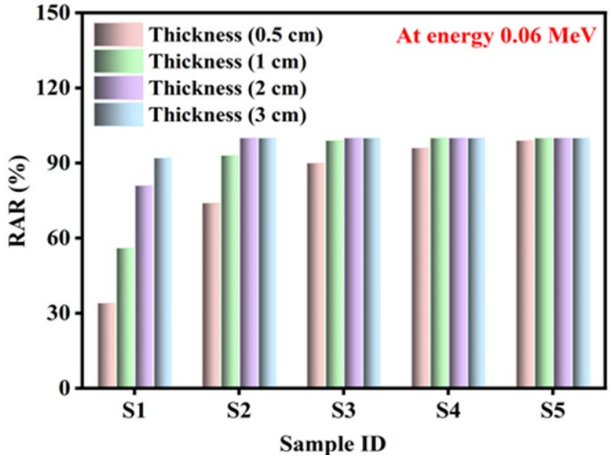

Fig. 9. The value of radiation absorption ratio (RAR) of the considered ceramic samples at energy 0.06 MeV for 0.5 cm, 1 cm, 2 cm, and 3 cm thicknesses.

Conclusion

Among the five MgO ceramic samples 0, 10, 20, 30, and 50 % of Barite ($BaSO_4$) have been contaminated instead of MgO termed as S1, S2, S3, S4, and S5 were calculated for few shielding parameters using Geant4 code and Experimental technique on the purpose of radiation shielding. No significant variation were found for the value of linear attenuation coefficients (LAC) of the considered ceramic samples calculated via Geant4 code and Experimental technique. Except ceramic sample S1 a sharp increase was found at energy 0.04 MeV representing value S1(10.6), S2(29.8), S3(38.3), S4(43), and S5(48.1). Considered ceramic samples S2, S3, S4, and S5 provided 3.2 times, 5.5 times, 7.7 times, and 12.8 times greater value of linear attenuation coefficients (LAC) than considered ceramic samples S1. As well as the considered ceramic sample S5 having composition [MgO (50%)-$BaSO_4$ (50%)] were presented lowest value of HVL, TVL, and MFP. According to the value of radiation absorption ratio (RAR), it has been found that ceramic sample S5 with a thickness of 0.5 cm can approximately prevent all of the incident photons at lower energy. Eventually, it can be said that with the greater enhancement of Barite ($BaSO_4$) uprise the shielding ability of considered MgO ceramic.

Acknowledgments

The authors express their gratitude to Princess Nourah bint Abdulrahman University Researchers Supporting Project number (PNURSP2023R57), Princess Nourah bint Abdulrahman University, Riyadh, Saudi Arabia

References

[1] Bulent Aktas, Abuzer Acikgoz, Demet Yilmaz, Serife Yalcin, Kaan Dogru, Nuri Yorulmaz. Journal of Nuclear Materials 563 (2022) 153619; https://doi.org/10.1016/j.jnucmat.2022.153619

[2] Melek Fidan, Abuzer Acikgoz, Gokhan Demircan, Demet Yilmaz, Bulent Aktas, Journal of Physics and Chemistry of Solids 163 (2022) 110543; https://doi.org/10.1016/j.jpcs.2021.110543

[3] A. T. Şensoy, H S. Gökçe, Construction and Building Materials, 253 (2020) 119218; https://doi.org/10.1016/j.conbuildmat.2020.119218

[4] Mengge Dong, Xiangxin Xue, He Yang, Dong Liu, Chao Wang, Zhefu Li, Journal of Hazardous Materials 318 (2016) 751-757; https://doi.org/10.1016/j.jhazmat.2016.06.012

[5] W. Chaiphaksa, P. Borisut, N. Chanthima, J. Kaewkhao, N.W. Sanwaranatee, Materials Today: Proceedings 65 (2022) 2412-2415; https://doi.org/10.1016/j.matpr.2022.05.529

[6] S. Kaewjaeng, S. Kothan, W. Chaiphaksa, N. Chanthima, R. Rajaramakrishna, H.J. Kim, J. Kaewkhao, Radiation Physics and Chemistry 160 (2019) 41-47; https://doi.org/10.1016/j.radphyschem.2019.03.018

[7] S. Kaewjaeng, N. Chanthima, J. Thongdang, S. Reungsri, S. Kothan, J. Kaewkhao, Materials Today: Proceedings, 43 (2021) 2544-2553; https://doi.org/10.1016/j.matpr.2020.04.615

[8] K.A. Naseer, G. Sathiyapriya, K. Marimuthu, T. Piotrowski, M.S. Alqahtani, E.S. Yousef, Optik (Stuttg). 251 (2022) 168436; https://doi.org/10.1016/j.ijleo.2021.168436

[9] M.I. Sayyed, K.A. Mahmoud, Optik 257 (2022) 168810; https://doi.org/10.1016/j.ijleo.2022.168861

[10] I.S. Mahmoud, Shams A.M. Issa, Yasser B. Saddeek, H.O. Tekin, Ozge Kilicoglu, T. Alharbi, M.I. Sayyed, T.T. Erguzel, Reda Elsaman, Ceramics International 45 (2019) 14058-14072; https://doi.org/10.1016/j.ceramint.2019.04.105

[11] I. Demir, M. Gümüş, H S. Gökçe, Construction and Building Materials, 257 (2020) 119596; https://doi.org/10.1016/j.conbuildmat.2020.119596

[12] Y. Al-Hadeethi, M.I. Sayyed, Progress in Nuclear Energy 129 (2020) 103511; https://doi.org/10.1016/j.pnucene.2020.103511

[13] S.A. Tijani, Y. Al-Hadeethi. Mater. Res. Express 6 (2019), 055323; https://doi.org/10.1088/2053-1591/ab0578

[14] A. Temir, K. Zhumadilov, M. Zdorovets, A. Kozlovskiy, A. Trukhanov, Solid State Sciences 115 (2021) 1106604; https://doi.org/10.1016/j.solidstatesciences.2021.106604

[15] A. Temir, K. Sh Zhumadilov, M.V. Zdorovets, A. Kozlovskiy, A.V. Trukhanov, Optical Materials 115 (2021) 111037; https://doi.org/10.1016/j.optmat.2021.111037

[16] Sinan Asal, Sema Akyil Erenturk, Sevilay Haciyakupoglu. Nuclear Engineering and Technology 53 (2021) 1634-1641; https://doi.org/10.1016/j.net.2020.11.009

[17] Berna Oto, Esra Kavaz, Halil Durak, Aydın Aras, Zekiye Madak. 2019, Ceramics International 45(17), 23681-23689; https://doi.org/10.1016/j.ceramint.2019.08.082

[18] M.I. Sayyed, E. Hannachi, Y. Slimani, Mayeen Uddin Khandaker, M. Elsafi, Radiation Physics and Chemistry 200 (2022) 110096; https://doi.org/10.1016/j.radphyschem.2022.110096

[19] M.H.A. Mhareb, Y. Slimani, Y.S. Alajerami, M.I. Sayyed, Eloic Lacomme, M.A. Almessiere. Ceramics International 46 (2020) 28877-28886; https://doi.org/10.1016/j.ceramint.2020.08.055

[20] E. Hannachi, K.A. Mahmoud, M.I. Sayyed, Y. Slimani, Materials Science in Semiconductor Processing 145; (2022), 106629; https://doi.org/10.1016/j.mssp.2022.106629

[21] V. Kozhukharov, M. Marinov, G. Grigorova, J. Non-Cryst. Solids, 28 (1978), pp. 429-430; https://doi.org/10.1016/0022-3093(78)90092-3

[22] H. Bürger, K. Kneipp, H. Hobert, W. Vogel, V. Kozhukharov, S. Neov. J. Non-Cryst. Solids, 151 (1992), pp. 134-142; https://doi.org/10.1016/0022-3093(92)90020-K

[23] M.Y.Hanfi, M.I.Sayyed, E.Lacomme, I.Akkurt, K.A.Mahmoud. Nuclear Engineering and Technology. 53, 6, 2021, 2000-2010; https://doi.org/10.1016/j.net.2020.12.012

[24] Singh KJ, Singh N, Kaundal, RS, Singh K., Nucl Instr Meth Phys Res B 2008; 266: 944-948; https://doi.org/10.1016/j.nimb.2008.02.004

[25] M. Mirzaei, M. Zarrebini, A. Shirani, M. Shanbeh, S. BorhaniTextil. Res. J., 89 (1) (2019), pp. 63-75; https://doi.org/10.1177/0040517517736475

[26] D.K. Gaikwad, M.I. Sayyed, S.N. Botewad, S.S. Obaid, Z.Y. Khattari, U.P. Gawai, F. Afaneh, M.D. Shirshat, P.P. Pawar. J. Non-Cryst. Solids, 503 (2019), pp. 158-168; https://doi.org/10.1016/j.jnoncrysol.2018.09.038

[27] S. Jaiyen, et al., Applied Mechanics and Materials. Trans Tech Publ (2017), pp. 204-207; https://doi.org/10.4028/www.scientific.net/AMM.866.204

[28] E. Kalkornsurapranee, et al., Radiat. Phys. Chem., 179 (2021), 109261; https://doi.org/10.1016/j.radphyschem.2020.109261

[29] Aloraini, D.A., Elsafi, M., Almuqrin, A.H., Sayyed, M.I., Science and Technology of Nuclear Installations, 2022, 5718920; https://doi.org/10.1155/2022/5718920

[30] Al-Ghamdi, H., Elsafi, M., Almuqrin, A.H., Yasmin, S., Sayyed, M.I., Materials, 2022, 15(15), 5310; https://doi.org/10.3390/ma15155310

[31] Al-Ghamdi, H., El-Nahal, M.A., Saleh, I.H., Sayyed, M.I., Almuqrin, A.H. Materials, 2022, 15(15), 5130; https://doi.org/10.3390/ma15155130

[32] Sayyed, M.I., Yasmin, S., Almousa, N., Elsafi, M., Processes, 2022, 10(9), 1725; https://doi.org/10.3390/pr10091725

[33] Sayyed, M.I., Hashim, S., Hannachi, E., Slimani, Y., Elsafi, M., Crystals, 2022, 12(11), 1602; https://doi.org/10.3390/cryst12111602

[34] J.F. Briesmeister, MCNP^< TM>-A General Monte Carlo N-Particle Transport Code, Version 4C, LA-13709-M. (2000).

[35] M.I. Abbas, M.S. Badawi, A.A. Thabet, Y.N. Kopatch, I.N. Ruskov, D.N. Grozdanov, S. Noureddine, N.A. Fedorov, M.M. Gouda, C. Hramco, others, Appl. Radiat. Isot. (2020) 109139; https://doi.org/10.1016/j.apradiso.2020.109139

[36] S. Hurtado, M. Garc\ia-León, R., Detect. Assoc. Equip. 518 (2004) 764-774; https://doi.org/10.1016/j.nima.2003.09.057

[37] M. I. Sayyed, O. I. Olarinoye and Mohamed Elsafi, Eur. Phys. J. Plus, 136 5 (2021) 535;

https://doi.org/10.1140/epjp/s13360-021-01492-y
[38] R. Brun, F. Rademakers, Detect. Assoc. Equip. 389 (1997) 81-86; https://doi.org/10.1016/S0168-9002(97)00048-X
[39] Aljawhara H. Almuqrin, M.I. Sayyed, M. Elsafi, Mayeen Uddin Khandaker, Radiation Physics and Chemistry. 2022,110170; https://doi.org/10.1016/j.radphyschem.2022.110170
[40] Dalal Abdullah Aloraini, M.I. Sayyed, K.A. Mahmoud, Aljawhara A.H. Almuqrin, Ashok Kumar, Mayeen Uddin Khandaker, Mohamed Elsafi, Radiation Physics and Chemistry. 2022, 110172; https://doi.org/10.1016/j.radphyschem.2022.110172
[41] Nuha Al-Harbi, M.I. Sayyed, Yas Al-Hadeethi, Ashok Kumar, M. Elsafi, K.A. Mahmoud, Mayeen Uddin Khandaker, D.A. Bradley, Radiation Physics and Chemistry. 188 (2021) 109645; https://doi.org/10.1016/j.radphyschem.2021.109645
[42] Ashwitha Nancy D'Souza, M.I. Sayyed, Naregundi Karunakara, Hanan Al-Ghamdi, Aljawhara H. Almuqrin, M. Elsafi, Mayeen Uddin Khandaker, Sudha D. Kamath, Radiation Physics and Chemistry. 2022, 110233; https://doi.org/10.1016/j.radphyschem.2022.110233
[43] M.I. Sayyed, M.F. Alrashedi, Aljawhara H. Almuqrin, M. Elsafi, Journal of Materials Research and Technology. 17 (2022) 2073-2083; https://doi.org/10.1016/j.jmrt.2022.01.113
[44] Yas Al-Hadeethi, M.I. Sayyed, Abeer Z. Barasheed, Moustafa Ahmed, M. Elsafi, Journal of Materials Research and Technology. 17 (2022) 223-233; https://doi.org/10.1016/j.jmrt.2021.12.109
[45] E. Hannachi, M.I. Sayyed, Yassine Slimani, M. Elsafi, Journal of Alloys and Compounds. 904 (2022) 164056.
[46] Sayyed, M.I.; Hamad, M.K.; Mhareb, M.H.A.; Kurtulus, R.; Dwaikat, N.; Saleh, M.; Elsafi, M.; Taki, M.M.; Kavas, T.; Ziq, K.A.; et al., Radiat. Phys. Chem. 2022, in press; https://doi.org/10.1016/j.jallcom.2022.164056